Phase Transition of II–VI Semiconductor Nanocrystals

ARTICLE *in* THE JOURNAL OF PHYSICAL CHEMISTRY C · AUGUST 2010

Impact Factor: 4.77 · DOI: 10.1021/jp1056545

2 AUTHORS, INCLUDING:

S. Li

Nanjing University of Science and Technol…

727 PUBLICATIONS **5,605** CITATIONS

SEE PROFILE

Phase Transition of II−VI Semiconductor Nanocrystals

S. Li and G. W. Yang*

State Key Laboratory of Optoelectronic Materials and Technologies, Nanotechnology Research Center, School of Physics & Engineering, Sun Yat-sen University, Guangzhou 510275, Guangdong, People's Republic of China

Received: June 18, 2010; Revised Manuscript Received: August 3, 2010

The phase transition is fundamental for understanding physical and chemical properties of materials. The phase transition at the nanometer scale is usually distinguished from that of the bulk counterpart. It is essential to pursue the basic physics involved in the phase transition on nanoscale for applications of nanomaterials. Herein, we have established an analytical thermodynamic model at the nanometer scale to study the phase transition of II−VI semiconductor nanocrystals, and revealed the size-dependent polymorphism behaviors of the phase transition. The physical origin of the size effects on the polymorphism behaviors of II−VI semiconductor nanocrystals was addressed on the basis of the contributions of surface energy and surface stress of nanocrystals to the total Gibbs free energy. It was found that the low surface energy and the small surface stress always predominate the thermal stability of nanostructures with the metastable phase. These results provided new insight into the fundamental understanding of the phase transition of II−VI semiconductor nanocrystals.

1. Introduction

Groups II−VI semiconductor nanocrystals have attracted great attention in current microelectronics and optoelectronics. It is well-known that the crystalline structure of semiconductor nanocrystals as well as size and shape can greatly affect their optical, electronic, and thermal properties.[1] Therefore, it becomes urgent to have a better understanding of the structural stability and the phase transitions of semiconductor nanocrystals for their applications.[2]

Generally, the semiconductor materials of II−VI have the cubic zinc belnde (ZB) and hexagonal wurtzite (WZ) structures, in which each atom is tetrahedral coordinated by atoms of the opposite species.[3] These two structures are identical, but for the stacking sequence of successive layers, with the ZB structure following an ABCABC... stacking and the WZ taking an ABABAB... arrangement.[4] Thus, the structural similarity and the attendant small difference in internal energies are manifested by the well-know WZ−ZB polytypism. Naturally, a number of binary semiconductors such as CdSe, CdTe, ZnS, and ZnSe can be prepared at ambient conditions in either form. Despite these structural and thermodynamic similarities between WZ and ZB, their spectroscopic characteristics are very different.[5−7]

Therefore, a better understanding of the dependence of nanocrystal structure on size and shape can provide significant information to design effective paths for synthesis of II−VI semiconductor nanocrystals with expected properties. In this paper, taking the contribution surface energy and the internal pressure induced by the surface stress to the total Gibbs free energy of system, we develop an analytical thermodynamic model at the nanometer scale to pursue the structural stability and the phase transition of II−IV semiconductor nanocrystals.

2. Theoretical Method

For most II−VI semiconductors such as ZnS, ZnSe, and CdTe, the bulk ZB structure is energetically more favorable than that of the WZ one.[8] However, it is energetically easier to form a WZ nanocrystal than to form a ZB one when the diameter (D) of nanocrytstals is within several nanometer scales (usually less than 5 nm).[9] Thermodynamically, there are some points where the curves of the Gibbs free energy (G) values of the WZ and ZB structures would cross each other in their phase diagram. Thus, the diameter of nanocrystals at these points could be interpreted as the critical diameter (D_c) for the phase transition between WZ and ZB. Note this does not mean that these energetically favorable phases would preferably form in experimental synthesis. However, the size-dependent phase stability of II−VI semiconductor nanocrystals remains poorly understood.[10]

It is well-known that two factors are the major driving force for the phase transition between stable and metastable structures of nanocrystals, i.e., the surface energy (γ) and the internal pressure (P_{in}) induced by the surface stress (f).[10,11] Systematic calculations and the comprehensive comparisons of their surface energies and surface stresses are still lacking. Therefore, in this work, we first carry out the thermodynamic calculations for II−VI semiconductor nanocrystals with various phases and then study their size-dependent phase stability.

A thermodynamic model of the phase transition of II−IV semiconductor nanocrystals is developed as follows. In general, a map of phase transitions can be generated by comparing the Gibbs free energy difference (ΔG) values of all possible structures, as a function of size (D), temperature (T), and pressure (P), and importantly, theoretical modeling is proving to be a very useful tool in this regard.[10,12−14] If the temperature is not considered, the relative phase stability can be determined by comparing the cohesive energy. Although the complicated $\Delta G(T, P, D)$ function cannot be easily considered for solid phases, a simple way is to distinguish separately the effects of T, P, and D on $\Delta G(T, P, D)$.[11] Thus, this can be realized by roughly defining that the $\Delta G(T, P, D)$ function is contributed by the sum of (i) the temperature-dependent Gibbs free energy difference of bulk crystals $\Delta G_v(T, 0, \infty)$, (ii) the size-dependent surface free energy difference $\Delta G_s(D)$, and (iii) the size- and

* Corresponding author, stsygw@mail.sysu.edu.cn.

10.1021/jp1056545
Published on Web 08/18/2010

TABLE 1: Comparison of the Ground State Parameters of Bulk II−VI Semiconductor Compounds Obtained Using GGA (a_1, E_c), Cited Experimental Results (a_2,)[a]

		a_1	a_2[49−52,34,47]	E_c
ZnO	WZ	$a = 3.28$	$a = 3.25$[49]	366
		$c = 5.296$	$c = 5.207$	
	ZB	$a = 4.624$	$a = 4.62$[50]	360
ZnS	WZ	$a = 3.843$	$a = 3.823$	288
		$c = 6.304$	$c = 6.260$	
	ZB	$a = 5.44$	$a = 5.345$	292.6
ZnSe	WZ	$a = 4.016$	$a = 3.996$[47]	255.4
		$c = 6.578$	$c = 6.556$	
	ZB	$a = 5.695$	$a = 5.677$	257.8
ZnTe	WZ	$a = 4.365$	$a = 4.273$	221.9
		$c = 7.163$	$c = 6.989$	
	ZB	$a = 6.188$	$a = 6.1037$	224.1
CdS	WZ	$a = 4.213$	$a = 4.136$[51]	272.2
		$c = 6.855$	$c = 6.714$	
CdSe	ZB	$a = 5.950$	$a = 5.818$	271.9
	WZ	$a = 4.367$	$a = 4.300$	249.3
		$c = 7.109$	$c = 7.011$	
	ZB	$a = 6.162$	$a = 6.052$	249.1
CdTe	WZ	$a = 4.678$	$a = 4.57$[52]	218.2
		$c = 7.72$	$c = 7.49$	
	ZB	$a = 6.629$	$a = 6.48$	219.0

[a] a is the lattice constant in Å, and E_c indicates the cohesive energy in kJ/mol.

pressure-dependent elastic energy difference $\Delta G_e(P, D)$ induced by P. Namely, the $\Delta G(T, P, D)$ function is given as[11]

$$\Delta G(T, P, D) = \Delta G_v(T, 0,\infty) + \Delta G_s(D) + \Delta G_e(P, D) \quad (1)$$

where $G_s(D)$ is induced by the existence of the dangling bonds of surface atoms or by internal energy difference between surface atoms and interior atoms.

The $\Delta G_s(D)$ function is thus determined by[11]

$$\Delta G_s(D) = \gamma_w A_w - \gamma_z A_z = 6(\gamma_w V_w - \gamma_z V_z)/D \quad (2)$$

where subscripts w and z show the corresponding structures of WZ and ZB. When the low-dimensional materials could be approximately considered as quasi-isotropic, γ values could be taken as an algebraic mean value of different facets. The corresponding gram atom surface area of a nanostructure A can be determined by $A = 6V/D$ where D is defined as diameter and V denotes the gram-atom volume. In eq 2, the temperature dependence of γ values is neglected for simplification.[15] Additionally, eq 2 has neglected the facet effect of nanocrystals on $\Delta G_s(D)$. In reality, nanocrystals have polyhedron shapes where some of them have evident anisotropy.[16] When this difference induces an error being more than 10% of the corresponding value, the mean values of γ and A from all existing facets are invalid.

$\Delta G_e(D)$ is calculated by

$$\Delta G_e(P, D) = P_w V_w - P_z V_z \quad (3)$$

In eq 3, $P = P_e + P_{in}$, where P_e denotes the external pressure and P_{in} shows an excess internal pressure, which is induced by the existence of surface stress and is not negligible when the considered material is at the nanometer scale.[17] When $P_e \approx 0$, $P = P_{in}$. This is the situation of nanocrystals. As $D \rightarrow \infty$, $P = P_e$ with $P_{in} = 0$, which shows the usual pressure effect on bulk crystals.

TABLE 2: Comparison of γ Values of II−VI WZ (110), (100), and (001) Surfaces in J/m^2 among Our Simulation Result:s γ_1, Using GGA-Pw91: γ_2, LDA-CAPZ: γ_3, Based on Equation 4; γ_4, Other Theoretical Results[a]

		γ_1	γ_2	γ_3	γ_4
ZnO	(100)	0.82	1.14	1.20	1.02[27]
	(110)	0.86	1.25	1.19	1.12[27]
ZnS	(100)	0.367	0.51	0.66	0.52[37]
	(110)	0.385	0.50	0.67	0.49[37]
ZnSe	(100)	0.253	0.44	0.54	
	(110)	0.276	0.46	0.55	
ZnTe	(100)	0.18	0.40	0.41	
	(110)	0.21	0.40	0.41	
CdS	(100)	0.41	0.48	0.52	0.28[53]
	(110)	0.43	0.51	0.55	0.29[53]
CdSe	(100)	0.38	0.36	0.45	0.46[23]
	(110)	0.27	0.40	0.46	0.50[23]
CdTe	(100)	0.17	0.29	0.35	
	(110)	0.18	0.33	0.32	

[a] $Z_s = 3$, $Z_b = 4$, $A_s^{100} = 2(3^{1/2})ac/3$, $A_s^{110} = 4(3^{1/2})ac/3$, a and c can be found in Table 1.

TABLE 3: Comparison of γ Values of II−VI ZB (110) Surfaces in J/m^2 among Our Simulation Results: γ_1, Using GGA-Pw91; γ_2, LDA-CAPZ; γ_3, Based on Equation 4; Other Theoretical Results, γ_4[a]

		γ_1	γ_2	γ_3	γ_4
ZnO	(110)	0.92	1.26	1.13	
ZnS	(110)	0.51	0.68	0.67	0.53[45]
ZnSe	(110)	0.33	0.55	0.53	
ZnTe	(110)	0.29	0.45	0.41	
CdS	(110)	0.35	0.53	0.54	
CdSe	(110)	0.27	0.42	0.45	
CdTe	(110)	0.20	0.34	0.35	

[a] $Z_s = 3$, $Z_b = 4$, $A_s = (6^{1/2}/4)(1 + \cos(\theta/2))a^2$, $\theta = 109.5$ is the band angle.

2.1. Theoretical Determination of Surface Energy of II−IV Semiconductor Nanocrystals. γ is defined as the difference between the free energy of a surface atom and that of an interior one for a solid, which is one of the basic qualities to describe the surface stabilities.[18] It is well-known that the low coordinated atoms in the surface shells of 2−3 atomic size increase the total energy of the nanoparticles and is the origin of the surface energy. The difference between the structures induced the different surface energy, which is one of the most important factors in the phase transition.

However, there is a dearth of experimental measurements of surface energy of nanocrystals, because there are many technological difficulties associated with the measurements.[19,20]

Although a number studies have already been undertaken by other authors on the surface structure of II−VI semiconductors,[21−29] a consistent set of surface energy calculations is required to provide a suitable input for the theoretical model. Presently, two theoretical models are adopted in this contribution, i.e., the traditional broken-bond model and the density functional theory (DFT) calculations.

The traditional broken-bond model is suggested to estimate the γ values. In our previous work, a modified formula is developed,[30,31]

$$\gamma = [2 - Z_S/Z_B - (Z_S/Z_B)^{1/2}]E_c/2N_0A_s \quad (4)$$

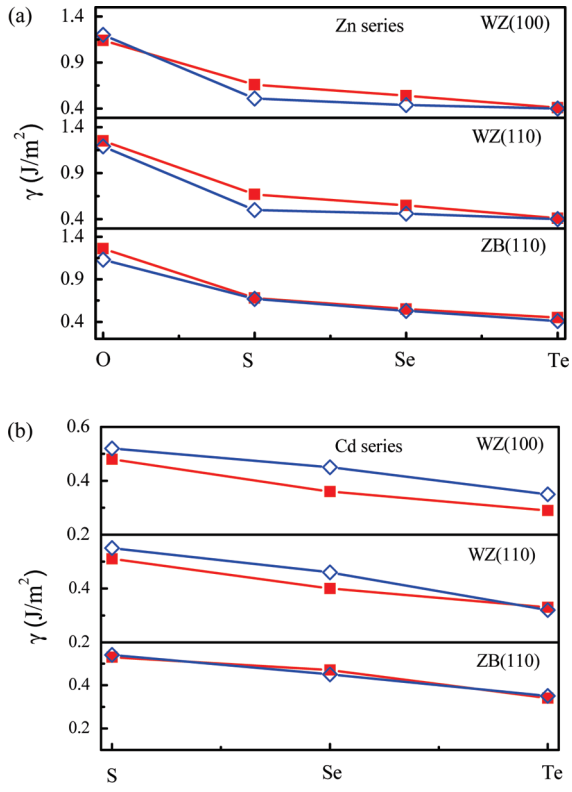

Figure 1. Comparison γ values of WZ (100) (110) and ZB (110) surfaces among simulation results using LDA (γ_2), eq 4 (γ_3): (a) Zn series materials; (b) Cd series materials. The symbols ■ and ◇ denote γ_2 and γ_3.

where Z_S and Z_B denote the coordination number (CN) of the surface atoms and the corresponding bulk atoms, respectively. N_0 is Avogadro's constant, and A_s is the mean atom surface. E_c is the cohesive energy. Due to its generality based on the bond broken rule, the model should be applicable for semiconductor compounds.[32] For the value of E_c in eq 4, the corresponding experimental values E_c should be utilized. However, E_c values of the considered compounds are incomplete and cannot be fully found in literature. Thus, to unify our calculations, the simulation results are taken in our calculations.

The γ values of II−VI semiconductor compounds can also be calculated using the DFT method. In addition, both the LDA-CAPZ and the generalized gradient approximation (GGA) functional with the PW91 method[33] are employed in this case. After geometry optimization, the bulk lattice constant a and E_c are obtained and listed in Table 1, in which we can see that our calculated results are in excellent agreement with previous reported data.[34]

Although the surface relaxation is inevitable, no surface reconstructions are detected in our studies. After relaxation, the cations move inward while the anions move outward, because of the charge transfer from the former to the latter.[34] For the surface calculations, the cutoff energy is set to 350 eV, and the k-points are 4 × 4 × 4. On the basis of these accuracy settings, the convergence tolerance of energy, maximum force, and maximum displacement becomes 2.0×10^{-5} eV/atom, 0.05 eV/Å, and 2.0×10^{-3} Å, respectively. To avoid the interaction between repeated slabs, a uniform vacuum width of 10 Å is employed. Therefore, the γ value is determined as follows[35]

$$\gamma = [E_{slab}(N) - NE_{bulk}]/2 \quad (5)$$

where $E_{slab}(N)$ is the total energy of an N-layer slab calculated with a sufficiently large value of N, and E_{bulk} denotes the bulk energy. The E_{bulk} values are determined by the slope of the $E_{slab}(N)$ values versus $N = 3, 5, 7$ using the method proposed by Boettger.[35]

2.2. Theoretical Determination of Surface Stress of II−IV Semiconductor Nanocrystals. By using the Laplace−Yong equation for a spherical nanocrystal with diameter D, the internal pressure P_{in} induced by the curvature can be expressed as

$$P_{in} = 4f/D \quad (6)$$

where f denotes the surface stress.[11,36] For nanocrystals, because the D value is very small, the value of P_{in} is very large, and so it cannot be neglected. Therefore, the smaller the diameter D, the larger the value of the internal pressure P_{in}.

f associated with the reversible work per unit area needed to elastically stretch a pre-existing surface is another surface quantity being different from γ. Since $d(\gamma A) = \gamma\, dA + A\, d\gamma$ and $dA = A\, d\varepsilon$, $f = \gamma + \partial\gamma/\partial\varepsilon$.[37] Up to now, there is not a general mathematical expression for the solid−gas interface f value, though this f value has been calculated case by case through some mechanical formulas.[11] Under the assumption that the fluid has no effect on the surface strain of solids, f_{sl} is considered to be identical with f, $f \approx f_{sl}$.[11]

The stress on solid−liquid interface f_{sl} has been expressed as[11]

$$f_{sl} = (hD_0S_{vib}H_mB/16VR)^{1/2} \quad (7)$$

where $D_0 = 3h$ for spherical nanocrystals, h is the mean diameter of atoms, B is the bulk modulus, S_{vib} is the vibrational part of the overall gram-atom melting entropy S_m, and $S_{vib} \approx S_m - R$ for most semiconductors,[38] and H_m is the melting enthalpy at the melting temperature.[11]

3. Results and Discussion

Table 1 compares our results of bulk parameters with those from experiments.[34] Tables 2 and 3 give the surface energy of WZ and ZB structures, in which γ_1 values are from the GGA-PW91 functional, γ_2 values are from the LDA-CAPZ functional, and γ_3 values are from eq 4 where E_c values in eq 4 are from our GGA simulation results. The cited theoretical data γ_4 are also shown for comparison purposes. Note that, LDA works better than GGA for the certain classes of systems and properties, in particular for calculating surface energies.[32,39] This is because LDA shows a better cancellation of errors between surface exchange and correlation energies.

In our surface energy calculations, only the (110) and (100) facets of WZ and the (110) facet of ZB structures have been considered. The reason is that the (110) surface seems to be the most important among all surfaces in the ZB II−VI semiconductors. According to literature, the crystal morphology of nanostructures with ZB phase is determined to be dodecahedron and only the (110) surface is present in the morphology because of its much higher stability.[40] The morphology of WZ phase has a cylindrical-like shape and is highly anisotropic, in which it has a large nonpolar area exposing the (110) and (100) surfaces and small areas closing the cylinder exposing the polar (001) and (00$\bar{1}$) surfaces.[40] To minimize the total free energy, the equilibrium crystal shape would develop. As a result, the crystal is bounded by the low surface energy facets. Therefore,

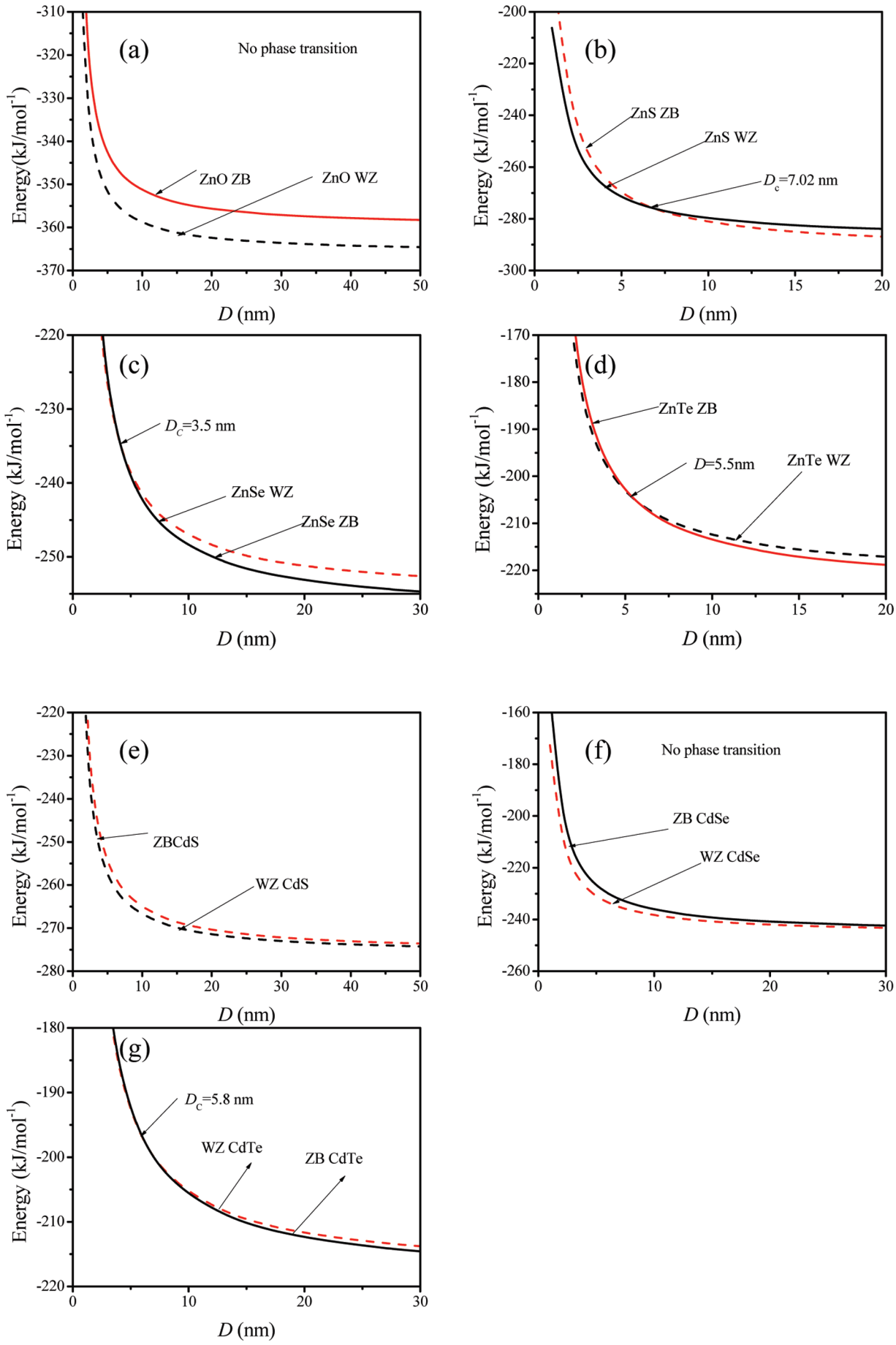

Figure 2. Free energy of formation for II−VI semiconductor nanocrystals with the WZ structure and ZB structures, as a function of the average diameter (D). The solid lines denote ZB, and dash lines denote WZ, (a) ZnO, (b) ZnS, (c) ZnSe, (d) ZnTe, (e) CdS, (f) CdSe, and (g) CdTe.

TABLE 4: Thermodynamic Data for Zn Series II−VI Semiconductor in Different Structures

	ZnO		ZnS		ZnSe		ZnTe	
	z	w	z	w	z	w	z	w
h (nm)[a]	0.200	0.166	0.236	0.197	0.247	0.205	0.268	0.223
V (cm^3 g-atom^{-1})[b]	7.42	7.17[54]	11.5	10.2	13.71[34]	13.6	16.33	16.6
H_m (kJ g-atom^{-1})[c]	9.2	9.34[55]	21.5[11]	15[11]	26.4[56]	24	31.5[57]	29.3
T_m (K)[d]	2243	2248[58]	2100[11]	1973[11]	1773	1718	1573	1465
S_m (J g-atom^{-1} K^{-1})[d]	4.15	4.15[58]	10.2	7.6	14.9	14.9	20	20
S_{vib} (J g-atom^{-1} K^{-1})	4.15	4.15[58]	10.2	7.6	6.59	6.59	11.69	11.69
B (GPa)[e]	198	142.6[58]	77.1[59]	74[59]	62.4	58.8	50.9	39.5
γ (J/m^2)[f]	1.26	1.19	0.68	0.50	0.55	0.45	0.45	0.40
f (J/m^2)[g]	0.96	0.69	1.31	0.94	1.04	0.85	1.35	0.81

[a] $h_w = a^2/(6c) + c/4$ where a and c are the lattice constants of the wurtzite structure, $h_z = 3^{1/2}a/4$ where a is the lattice constant of the zinc blende structure.[36] [b] $V_g = N_0\upsilon_a$ where N_0 is the Avogadro's constant and υ_a the mean atom volume in the corresponding crystalline structure. $\upsilon_{aw} = 3^{1/2}a^2c/8$ and $\upsilon_{aZ} = a^3/8$. [c] Since $\Delta H \approx H_{mz} - H_{mw}$ where ΔH is the transitional enthalpy between wurtzite and zinc blende phases of the crystal; H_{mw} and H_{mz} are melting temperatures of the both phases, the H_{mz} value is determined by $H_{mz} = \Delta H + H_{mw}$. [d] As a first-order approximation, $S_{mz} \approx S_{mw}$ and thus $T_m = H_m/S_m$. As a first-order approximation $\Delta H \approx \Delta E$, ΔE is the difference of cohesive energy between WZ and ZB. [e] Some value of bulk modulus have no experimental results, we used DFT calculated the absent ones. [f] For WZ phase the $\gamma = \gamma_{100} + \gamma_{110}$, and for ZB phase the $\gamma = \gamma_{110}$. Here we used the γ_2 in Table 2 and 3. [g] f is determined by eq 7.

the mean γ value of nanocrystals in light of the above consideration is a determined algebraic sum.

From Tables 2 and 3, we can see that our LDA results are in agreement with those from the modified broken bond model. Although the absolute values are somewhat different, the same orders can always be found from different methods, as shown in Figure 1. In detail, in the Zn series, γ values decrease along the sequence going from O to Te. After bond cutting, the energy loss of ZnO is the largest, while ZnTe is the smallest. Thus, these results prove again that the variations of γ are consistent with the corresponding E_c values.

Comparing the results of LDA and the modified broken bond model, we can see that, for the ZB (110), the surface energy values obtained by the two models agree very well. It is well-known that if surfaces are fully relaxed without any symmetry constraints, bond lengths and angles all change. Thus, after relaxation, the regular surfaces become deformed. Although the modified broken bond model has been improved,[33] the mean atom surface A_s caused by the surface deformation in eq 4 still cannot be considered. Therefore, from the cited results, we can see that the modified broken bond model is more simple and LDA is more accurate for surface energy calculations.

Figure 2 has shown the total energy of different phases of WZ or ZB as a function of diameter of nanocrystals based on eq 1. The used parameters in our calculations are listed in Tables 4 and 5. Clearly, we can see that the energy increases with the diameter decreasing. Since the small diameter causes the large surface/volume ratio for nanostructures, the γ and the internal pressure P_{in} effects become more and more important for nanomaterials. We have studied seven kinds of nanocrystals, such as ZnO, ZnS, ZnSe, ZnT, CdS, CdSe, and CdTe in this case. For all these nanocrystals, the WZ structure has lower γ and f than that of the ZB structure. From Table 1, we can see that WZ is the stability phase for ZnO, CdS, and CdSe, and the size decrease cannot induce the phase transition from WZ to ZB. Then in parts a, e, and f of Figure 2, the total energy of the WZ phase is always lower than that of the ZB one, which means that WZ is the stable phase and ZB is the metastable phase. Note that there is no agreement on which phase is stable for the bulk CdSe.[41] Therefore, we also calculate the cohesive energy values using GGA-PW91, and the result shows that the WZ phase has lower energy.

ZnS, ZnSe, and ZnTe crystals have both the ZB and WZ structures, in which the ZB is stable[42] and the WZ is metastable. For example, some WZ-type ZnS and ZnSe nanocrystals have been synthesized using some techniques including the precursor decomposition via solvothermal reactions, ultrasonication, and colloide.[43−46]

TABLE 5: The Thermodynamic Data of Cd Series II−VI Semiconductor in Different Structures

	CdS		CdSe		CdTe	
	z	w	z	w	z	w
h (nm)[a]	0.258	0.215	0.267	0.219	0.287	0.240
V (cm^3 g-atom^{-1})[a]	14.8[62]	15.1[60]	16.7	16.9	20.5	20.4
H_m (kJ g-atom^{-1})	24.1	25.1	23.4	22.8[11]	25.2[60]	24.3
T_m (K)	1678[61]	1748	1563[11]	1525	1371	1318
S_m (J g-atom^{-1} K^{-1})	14.36	14.36	14.94	14.96	18.4	18.4
S_{vib} (J g-atom^{-1} K^{-1})	6.05	6.05	6.62	6.62	10.1	10.1
B (GPa)	66[62]	62.7[63]	53.1[62]	45.6[64]	44.5[65]	39.3
γ (J/m^2)	0.53	0.50	0.17	0.38	0.34	0.31
γ	0.53	0.48	0.17	0.36	0.34	0.29
f (J/m^2)	0.99	0.81	0.69	0.54	1.02	0.77

[a] $h_w = a^2/(6c) + c/4$ where a and c are the lattice constants of the wurtzite structure, $h_z = 3^{1/2}a/4$ where a is the lattice constant of the zinc blende structure.[11,34] [b] $V_g = N_0\upsilon_a$ where N_0 is the Avogadro's constant and υ_a the mean atom volume in the corresponding crystalline structure. $\upsilon_{aw} = 3^{1/2}a^2c/8$ and $\upsilon_{aZ} = a^3/8$. [c] Since $\Delta H \approx H_{mz} - H_{mw}$ where ΔH is the transitional enthalpy between wurtzite and zinc blende phases of the crystal; H_{mw} and H_{mz} are melting temperatures of both phases, H_{mz} value is determined by$H_{mz} = \Delta H + H_{mw}$. [d] As a firstorder approximation, $S_{mz} \approx S_{mw}$ and thus $T_m = H_m/S_m$. As a first-order approximation $\Delta H \approx \Delta E$, ΔE is the difference of cohesive energy between WZ and ZB. [e] Some value of bulk modulus have no experimental results, we used DFT calculated the absent ones. [f] For WZ phase the $\gamma = \gamma_{100} + \gamma_{110}$, and for ZB phase the $\gamma = \gamma_{110}$. Here we used the γ_2 in Tables 2 and 3. [g] f is determined by eq 7.

For ZnS, ZnSe, ZnTe, and CdTe, ZB is the bulk stable phase. For example, the bulk crystalline structure of CdTe is the ZB type. Then, at the nano regime, Murray et al. reported the stabilization of the hexagonal CdTe nanocrystals for the first time using dimethylcadmium as cadmium source.[47] On the basis of eqs 1−3), ΔG between WZ and ZB decreases with the D decreasing. However, there exists a critical size D_c, and at $D = D_c$, $\Delta G = 0$, which means that the WZ and ZB phase have the equation energy. When $D < D_c$, the WZ become thermodynamically stable. Thus, from panels b, c, d, and g of Figure 2, we can see that $D_c = 7.02$, 3.5, 5.5, and 5.8 nm for ZnS, ZnSe, ZnTe, and CdTe, respectively. Therefore, ZB is stable and WZ is metastable when $D > D_c$. From Tables 4 and 5, it is observed that the γ and f values of the WZ II−VI nanocrystals are lower

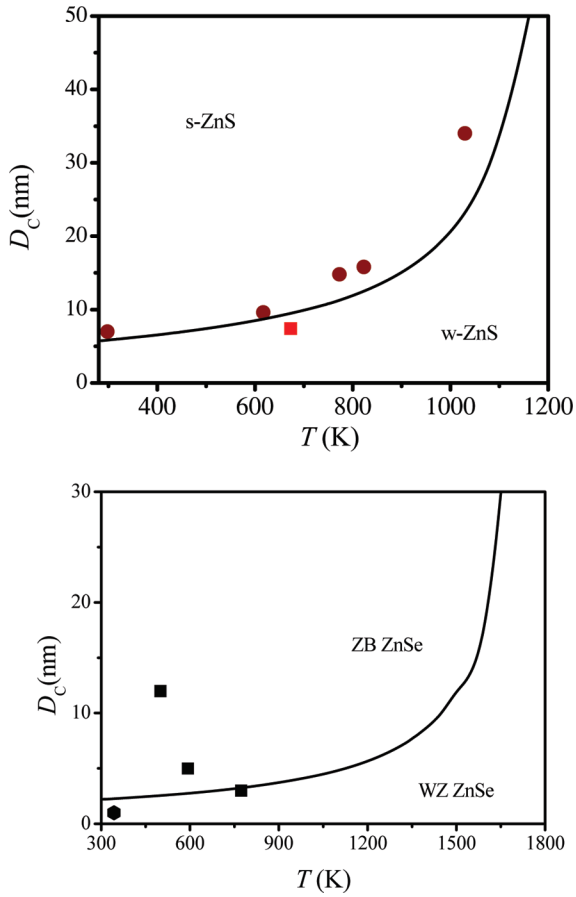

Figure 3. $D_c(T)$ functions of ZnS and ZnSe for nanocrystals in terms of eqs 1 (20 and (3) (solid line). (a) The symbols ■[66] and ●[13] show the corresponding experimental results for ZnS nanocrystals. Some necessary data in eq 1 and related equations are given as follows. In eq 1, $\Delta H = 6.5$ kJ g-atom^{-1}.[11] Other related parameters used in eq 1 and related equations are shown in Table 5. For semiconductors, $\Delta G_m(T) = \Delta H_m T(T_m - T)/T_m^2$ with ΔH_m being the bulk melting enthalpy at T_m.[67] (b) The symbols ⬣[44−46] and ■[43] show the corresponding experimental results for ZnS nanocrystals. Some necessary data in eq 1 and related equations are given as follows. In eq 1, as a first-order approximation, $\Delta H \approx \Delta E = 2.4$ kJ g-atom^{-1}. Other related parameters used in eq 1 and related equations are shown in Table 5.

than those of the ZB, which leads to the stabilization of the WZ structure as D decreases.

Although the polar surfaces have been shown to be very effective in the prediction of solid state and surface properties and that can be extended to nucleation and growth phenomena, we must point out that the polar surfaces have not been considered in our studies. We assume that all the nanoparticles were ideal; all the facets were the surface with lowest energy. In reality, the appearance of the polar surface must have effects on the phase stability and phase transition. When this difference induces an error being more than 10%, the assumption is invalid.

Thus, the mean surface energy γ_w has been underestimated. If the polar surfaces are considered, the obtained D_c would smaller than that we determined. Therefore, the WZ nanocrystals are difficult to prepare in experimental.

On the basis of these theoretical results, we can easily see that, for the ZnSe nanocrystals, the WZ phase seems difficult for experimental synthesis. However, the ZnSe nanowires with the WZ phase can be prepared.[48] The reason is that, for the WZ nanowires, the surface is the (110), and each of the atoms consists of three coordinated atoms. Then for the ZB structure, each of atoms consists of two or three coordinated atoms. Thus, the presence of two-coordinated atoms leads to a high surface dangling bonds ratio in the ZB structures compared with that in the WZ structures with close D.[48] Meanwhile, $\Delta\gamma = \gamma_z - \gamma_w$ increases as the diameter of nanowires decreasing, while increases the driver force of phase transition.

Additionally, we need emphasize that D_c is temperature-dependent. D_c values are obtained at $T = 300$ K in the calculations above. On the basis of eqs 1−3, the temperature-dependent D_c functions of ZnS and ZnSe are plotted in Figure 3, in which the used parameters are listed in Table 4. Clearly, D_c monotonically increases as the temperature increasing, which means that the high temperature benefits the WZ structure's stability. In Figure 3a, the signs are the theoretical simulations, which denote the phase transition point. In Figure 3b, the signs are the experimental results, which denote the synthesis of nanocrystals.

4. Conclusion

In summary, we have provided a comprehensive understanding of the phase transition of II−VI semiconductor nanocrystals by an analytical thermodynamic model on the basis of first-principles calculations. The surface energies of II−VI semiconductor nanocrystals have been systemically calculated using the modified broken bond model and the DFT method. It was found that the WZ phase become thermodynamically stable as the size of nanocrystals decreases for ZnS, ZnSe, ZnTe, and CdTe, and the phase transition size is temperature-dependent. The theoretical results are consistent with the available experimental data and other calculations, which implied that these theoretical methods are applicable to nanomaterials.

Acknowledgment. This work was supported by NSFC (U0734004 and 10974260), the Ministry of Education, and the Postdoctoral Science Foundation of China (20090460794).

References and Notes

(1) Karki, B. B.; Wentzcovitch, R. M. *Phys. Rev. B* **2003**, *68*, 224304.
(2) Alivisatos, A. P. *J. Phys. Chem. B* **1996**, *100*, 13227.
(3) Wyckoff, R. W. G. *Crystal Structure*, 2nd ed.; Interscience: New York, 1963.
(4) Harrison, W. A. *Electronic Structure and the Properties of Solid*; Freeman: San Francisco, 1980; pp 229−256.
(5) Fedorov, V. A.; Ganshin, V. A.; Korkishko, Y. N. *Phys. Status Solidi A* **1991**, *126*, K5.
(6) Murray, C. D.; Norris, D. J.; Bawendi, M. G. *J. Am. Chem. Soc.* **1993**, *115*, 8706.
(7) Li, S.; Li, J. L.; Jiang, Q.; Yang, G. W. *J. Appl. Phys.* **2010**, *108*, 024102.
(8) Ma, C.; Moore, D.; Ding, Y.; Li, J.; Wang, Z. L. *Int. J. Nanotechnol.* **2004**, *1*, 431.
(9) Kumar, S.; Nann, T. *Small* **2006**, *2*, 316.
(10) Wang, C. X.; Yang, G. W. *Mater. Sci. Eng. R* **2005**, *49*, 157.
(11) Jiang, Q.; Li, S. *J. Comput. Theor. Nanosci.* **2008**, *5*, 2346.
(12) Campbell, C. T.; Parker, S. C.; Starr, D. E. *Science* **2002**, *298*, 811.
(13) Lupis, C. H. P. *Chemical Thermodynamics of Materials*; North Holland: North Holland: New York, 1983).
(14) Barnard, A. S.; Zapol, P. *J. Chem. Phys.* **2004**, *121*, 4276.
(15) Zhang, H. Z.; Huang, F.; Gilbert, B.; Banfield, J. F. *J. Phys. Chem. B* **2003**, *107*, 13051.
(16) Barnard, A. S. *J. Mater. Chem.* **2006**, *16*, 813.
(17) Blakely, J. M. *Introduction to the Properties of Crystal Surfaces*, 1st ed.; Pergamon Press: Oxford, 1973.
(18) Jiang, Q.; Lu, H. M.; Zhao, M. *J. Phys.: Condens. Matter* **2004**, *16*, 521.
(19) Ouyang, G.; Tan, X.; Yang, G. W. *Phys. Rev. B* **2006**, *74*, 195408.
(20) Renaud, G. *Surf. Sci. Rep.* **1998**, *32*, 5.
(21) Rempel, J. Y.; Trout, B. L.; Bawendi, M. G.; Jensen, K. F. *J. Phys. Chem. B* **2005**, *109*, 19320.
(22) Kresse, G.; Dulub, O.; Diebold, U. *Phys. Rev. B* **2003**, *68*, 245409.
(23) Csik, I.; Russo, S. P.; Mulvaney, P. *Chem. Phys. Lett.* **2005**, *414*, 322.

(24) Barnard, A. S.; Xu, H. F. *J. Phys. Chem. C* **2007**, *111*, 18112.
(25) Wang, Y. R.; Duke, C. B. *Phys. Rev. B* **1998**, *37*, 6417.
(26) Manna, L.; Wang, L. W.; Cingolani, R.; Alivisatos, A. P. *J. Phys. Chem. B* **2005**, *109*, 6183.
(27) Cooke, D. J.; Marmier, A.; Parker, S. C. *J. Phys. Chem. B* **2006**, *110*, 7985.
(28) Meyer, B.; Marx, D. *Phys. Rev. B* **2003**, *67*, 035403.
(29) Swank, R. K. *Phys. Rev.* **1967**, *135*, 844.
(30) Jiang, Q.; Lu, H. M. *Surf. Sci. Rep.* **2008**, *63*, 427.
(31) Liu, D.; Lu, H. M.; Jiang, Q. *J. Phys.: Condens. Matter* **2009**, *21*, 198002.
(32) Liu, W.; Zheng, W. T.; Jiang, Q. *Phys. Rev. B* **2007**, *75*, 235322.
(33) Perdew, J. P.; Wang, Y. *Phys. Rev. B* **1992**, *45*, 13244.
(34) Adachi, S. D. *Properties of Group-IV, III-V and II-VI Semiconductors*; John Wiley & Sons, Ltd: Hoboken, NJ, 2005; p 7.
(35) Boettger, J. C. *Phys. Rev. B* **1994**, *49*, 16798.
(36) Cammarata, C. R.; Sieradazki, K. *Annu. Rev. Mater. Sci.* **1994**, *24*, 215.
(37) Zhang, H. Z.; Oenn, R. L.; Hamers, R. J.; Banfield, J. F. *J. Phys. Chem. C* **1999**, *103*, 4656.
(38) Regel', A. R.; Glazov, V. M. *Semiconductor* **1995**, *29*, 405.
(39) Mattsson, A. E.; Schultz, P. A.; Desjarlais, M. P.; Mattsson, T. R.; Leung, K. *Modell. Simul. Mater. Sci. Eng.* **2005**, *13*, R1.
(40) Hamad, S.; Cristol, S.; Catlow, C. R. A. *J. Phys. Chem. B* **2002**, *106*, 11002.
(41) Fedorov, V. A.; Ganshin, V. A.; Korkishko, Y. N. *Phys. Status Solidi A* **1991**, *126*, K5.
(42) Wang, Z.; Daemen, L. L.; Zhao, Y.; Zha, C. S.; Downs, R. T.; Wang, X.; Wang, Z. L. *Nat. Mater.* **2005**, *4*, 922.
(43) Kumar, P.; Sngh, K. *J. Optoelectron. Biomed. Mater.* **2009**, *1*, 59.
(44) Rafea, M. A. *J. Mater. Sci.: Mater. Electron.* **2007**, *18*, 415.
(45) Zhu, J. J.; Koltypin, Y.; Gedanken, A. *Chem. Mater.* **2000**, *12*, 73.
(46) Cozzoli, P. D.; Manna, L.; Curri, M. L.; Kudera, S.; Ciannini, C.; Striccoli, M.; Agostiano, A. *Chem. Mater.* **2005**, *17*, 1296.
(47) Chen, M. H.; Gao, L. *Mater. Chem. Phys.* **2005**, *91*, 437.
(48) Li, S.; Yang, G. W. *Appl. Phys. Lett.* **2009**, *95*, 073106.
(49) Kresse, G.; Dulub, O.; Diebold, U. *Phys. Rev. B* **2003**, *68*, 245409.
(50) Oshikiri, M.; Aryasetiawan, F. *Phys. Rev. B* **1999**, *60*, 10754.
(51) Madelung, O.; Schulz, M.; Weiss, H. *Numerical Data and Functional Relationships in Science and Technology*; Springer-Verlag: Berlin, 1982; Vol. 176.
(52) Kumar, S.; Ade, M.; Nann, T. *Chem.—Eur. J.* **2005**, *11*, 2220.
(53) Barnard, A. S.; Xu, H. F. *J. Phys. Chem. C* **2007**, *111*, 18112.
(54) Karzel, H.; Potzel, W.; Kofferlein, M. *Phys. Rev. B* **1996**, *53*, 11425.
(55) Weast, R. C. *Handbook of Chemistry and Physics*, 69th ed.; Chemical Rubber Co: Cleveland, OH, 1988−1989; p B-227.
(56) Kobzar, V. A.; Konovalov, O. M. *Ukr. Khim. Zh.* **1983**, *49* (12), 1242−1244.
(57) Nasar, A.; Shamsuddin, M. *J. Less-Common Metals* **1990**, *161*, 93.
(58) Li, S.; Wen, Z.; Jiang, Q. *Scr. Mater.* **2009**, *59*, 526.
(59) Qadri, S. B.; Skelton, E. F.; Dinsmore, A. D.; Hu, J. Z.; Kim, W. J.; Nelson, C.; Ratna, B. R. *J. Appl. Phys.* **2001**, *89*, 115.
(60) Amzil, A.; Mathieu, J. C.; Castanet, R. *J. Alloys Compd.* **1997**, *256*, 192.
(61) Goldstein, A. N.; Ether, C. M.; Alivisatos, A. P. *Science* **1992**, *256*, 1425.
(62) Wright, K.; Gale, J. D. *Phys. Rev. B.* **2004**, *70*, 035211.
(63) Cohen, M. L. *Phys. Rev. B* **1985**, *32*, 7988.
(64) Rabani, E. *J. Chem. Phys.* **2002**, *116*, 258.
(65) *Landolt-Borstein Numerical Data and Functional Relationships in Science and Technology*; Madelung, O., Schulz, M., Weiss, H., Eds.; Springer-Verlag: Berlin, 1982; Vol. 17.
(66) Qadri, S. B.; Skelton, E. F.; Hsu, D.; Dinsmore, A. D.; Yang, J.; Gray, H. F.; Ratan, B. R. *Phys. Rev. B* **1999**, *60*, 9191.
(67) Hoffman, J. D. *J. Chem. Phys.* **1958**, *29*, 1192.

JP1056545